Estimating a fluctuating magnetic field with a continuously monitored atomic ensemble

Cheng Zhang[1,2] and Klaus Mølmer[2,*]

[1]*Department of Physics, Beijing Normal University, 100875 Beijing, China*
[2]*Department of Physics and Astronomy, University of Aarhus, DK-8000 Aarhus C, Denmark*

We study the problem of estimating a time-dependent magnetic field by continuous optical probing of an atomic ensemble. The magnetic field is assumed to follow a stochastic Ornstein-Uhlenbeck process and it induces Larmor precession of the atomic ground-state spin, which is read out by the Faraday polarization rotation of a laser field probe. The interactions and the measurement scheme are compatible with a hybrid quantum-classical Gaussian description of the unknown magnetic field, and the atomic and field variables. This casts the joint conditional quantum dynamics and classical parameter estimation problem in the form of update formulas for the first and second moments of the classical and quantum degrees of freedom. Our hybrid quantum-classical theory is equivalent to the classical theory of Kalman filtering and to the quantum theory of Gaussian states. By reference to the classical theory of smoothing and with the quantum theory of past quantum states, we show how optical probing after time t improves our estimate of the value of the magnetic field at time t, and we present numerical simulations that analyze and explain the improvement over the conventional filtering approach.

I. INTRODUCTION

The quantum parameter estimation combines elements of classical estimation theory with quantum measurement theory to provide estimates of classical parameters or signals conditioned on the outcome of measurements on quantum systems [1]. In cases where probing is accomplished by measurements on a quantum probe, classical Kalman filter theory can thus be combined with the density matrix formalism to describe hybrid quantum-classical components, and yield the maximum likelihood estimator of classical variables.

The estimation of a weak classical magnetic field is of both theoretical and practical interest in high-precision metrology. Atomic gases are excellent magnetic probes due to the Larmor precession of the atomic spin, which can be probed by a laser field [2]. The same probing, in turn, squeezes the collective atomic spin degree of freedom [3] and improves the precision compared to the standard counting statistics limits of independent probe atoms. The problem can be treated by Kalman filter theory [4,5]. For a recent, combined theoretical and experimental study, see [6]. In [7,8], a hybrid quantum-classical Gaussian-state formalism was proposed where the atomic and photonic degrees of freedom, as well as an unknown constant magnetic field, were treated as harmonic oscillator quadrature variables. In the absence of atomic dissipation, the effect of atomic spin squeezing led to a $1/T^3$ rather than $1/T$ time dependence of the variance of the estimate of a constant magnetic field. Atomic dissipation can be included in the formalism [9] and limits the degree of squeezing and prevents the long-time $1/T^3$ resolution.

In [7,10], the theory was generalized to the case of a magnetic field that fluctuates according to an Ornstein-Uhlenbeck (OU) process, and for which a hybrid Gaussian quantum-classical distribution still applies. This Gaussian distribution function is fully determined by the quadrature expectation values and covariances, which are evolving due to the interaction Hamiltonian and conditioned on the measurement outcomes until time t. In [10], it was speculated and proven that the use of measurement data acquired also after time t could be employed to improve, in hindsight, the estimate of the value of the magnetic field at the earlier time t.

For continuously monitored systems, *filtering* refers to the estimation of a classical signal at time t conditioned upon observations until time t, while *smoothing* refers to estimation of the same quantity based on observations both before and after t. In classical estimation theory, the forward Kalman-Bucy filter thus represents the Bayesian updating with time of our knowledge by the acquisition of new data. The combination of forward and backward filters in the so-called Mayne-Fraser-Potter two-filter smoother uses all data for a better estimate and is also an integral component of Kalman filter theory [4,11]. In [12–16], Tsang showed how estimation by both classical filtering and smoothing can be generalized to the case of Gaussian quantum probes. In the present article, we shall present an alternative derivation with a starting point in quantum measurement theory, i.e., quantum trajectories [17–20] and the past quantum state theory [21]. The two approaches yield identical results when the systems are restricted to Gaussian phase-space distributions, while our quantum approach may also be readily adapted to more general cases, which have their classical counterparts in the so-called forward-backward or $\alpha - \beta$ analysis of Hidden Markov Models [22–24].

The article is outlined as follows. In Sec. II, we introduce the atomic magnetometer and we describe how its dynamics

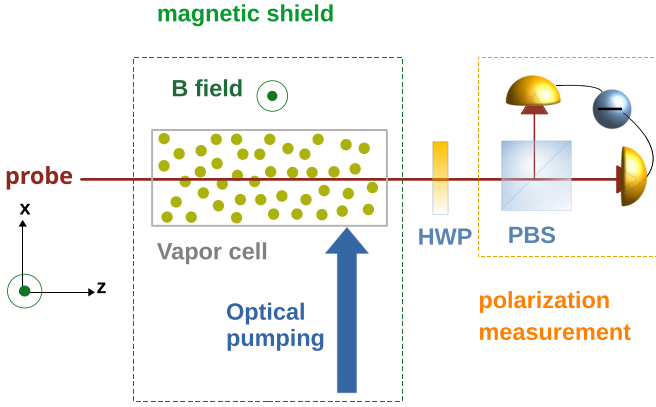*Corresponding author: moelmer@phys.au.dk

FIG. 1. Schematic of the physical setup. The atomic spins are polarized along the x axis by optical pumping. A B field along the y axis causes a Larmor precession of the atomic spins toward the z axis. By the Faraday interaction, the z component of the atomic spins causes rotation of the polarization of the probe field, which is detected by intensity measurements of suitable linear polarization components.

is captured by a few-mode harmonic oscillator description. In Sec. III, we present the Gaussian-state description of the unknown magnetic field and the collective quantum state of the atoms subject to optical probing. In Sec. IV, we derive the Gaussian-state mean values and covariance matrix for the smoothing, or past quantum state, analysis of the measurement record. In Sec. V, we present the numerical results of our schemes and address their performance in different limits. Section VI summarizes the paper and provides an outlook.

II. AN ATOMIC ENSEMBLE MAGNETOMETER

In this article, we model a unidirectional time-dependent magnetic field $B(t)$ by an Ornstein-Uhlenbeck process, governed by a stochastic equation

$$dB(t) = -\gamma_b B(t)dt + \sqrt{\sigma_b}dW, \qquad (1)$$

where dW is an infinitesimal Wiener increment with mean value 0 and variance dt. An example of $B(t)$ is shown by the solid green curve in Fig. 2. The associated probability distribution for the unknown value of the magnetic field obeys a Fokker-Planck equation with constant friction and diffusion terms, and an initial Gaussian distribution will remain Gaussian for later times.

An ensemble of spin-polarized atoms in a physical setup, such as the one shown in Fig. 1, permits real-time tracking of a time-dependent magnetic field $B(t)$. We assume N_{at} identical two-level atoms described by the Pauli spin matrices $\boldsymbol{\sigma}_i$ for the ith atom. We further assume that the atomic gas is dilute so that scattering and interactions among the atoms are negligible. The atoms are prepared by optical pumping in the same internal quantum state, spin polarized along the x direction. Mathematically, this allows us to treat the collective polarization along the x axis classically $\langle J_x \rangle = N_{at}/2$, ($\hbar = 1$), while the off-axis polarization components are quantum degrees of freedom and satisfy the commutation relation $[J_y, J_z] = iJ_x$. This inspires us to introduce the effective canonical coordinate and momentum variables $x_{at} =$

$J_y/\sqrt{\langle J_x \rangle}$, $p_{at} = J_z/\sqrt{\langle J_x \rangle}$ with the standard commutation relation $[x_{at}, p_{at}] = i$.

In the presence of the external magnetic field B, polarized along the y direction (see Fig. 1), the collective spin precesses toward the z axis, which in terms of the canonical atomic variables corresponds to the time evolution,

$$p_{at} \mapsto p_{at} - \mu\tau B, \qquad (2)$$

during each infinitesimal time interval τ, where $\mu = \beta\sqrt{\langle J_x \rangle}$ is given by the magnetic moment β. Note that we assume a weak magnetic field and short timescales so that the spin precession due to the B field subtends a very small angle and the linear approximation (2) applies throughout the probing process.

In addition, the atoms interact with a continuous, linearly polarized (along x) probe beam of light. The Faraday interaction causes a rotation of the optical polarization that is proportional with the atomic spin component J_z [8]. We adopt a simple description of the light-matter interaction by discretizing the beam into a sequence of segments of light with duration τ. The Stokes operator for each segment of light with N_{ph} photons has an x component which is effectively classical, $\langle S_x \rangle = N_{ph}/2$, while we may introduce the scaled canonical variables for the other two Stokes vector components, $x_{ph} = S_y/\sqrt{\langle S_x \rangle}$, $p_{ph} = S_z/\sqrt{\langle S_x \rangle}$, satisfying the commutation relation $[x_{ph}, p_{ph}] = i$. Following [8], the light-matter interaction in the Heisenberg picture is given by the two update rules

$$x_{at} \mapsto x_{at} + \kappa\sqrt{\tau}p_{ph}, \quad p_{at} \mapsto p_{at}, \qquad (3)$$

$$x_{ph} \mapsto \kappa\sqrt{\tau}p_{at} + x_{ph}, \quad p_{ph} \mapsto p_{ph}, \qquad (4)$$

where we introduce the coupling constant $\kappa = (d^2\omega/\Delta Ac\epsilon_0)\sqrt{N_{at}\Phi}$, with d the atomic dipole moment, ω the photon frequency, Δ the detuning from atomic resonance, A the area of the cross section of the light field, and $\Phi = N_{ph}/\tau$ the photon flux [25]. The dynamics of the atom and field variables is thus described by the effective Hamiltonian

$$H\tau = \kappa\sqrt{\tau}p_{at}p_{ph} + \mu\tau Bx_{at}, \qquad (5)$$

where we recall that a new segment of light enters at each new time interval of duration τ. Note that the atom-light interaction term in (5) is of the order of $\sqrt{\tau}$, which reflects the dependence of the vacuum field strength on the quantization volume of $A \cdot c\tau$.

III. GAUSSIAN-STATE FORMALISM FOR ESTIMATING A TIME-DEPENDENT NOISY MAGNETIC FIELD

The Hamiltonian (5) and the Ornstein-Uhlenbeck process (1) determine the evolution of the joint probability distribution of the magnetic field and the atomic and optical quadrature variables. This is accomplished by a density matrix $\rho(t) = \int dB|B\rangle\langle B| \otimes \rho_B(t)$, in which the different candidate values B of the classical magnetic field are treated as if they were eigenvalues of a quantum observable with eigenstates populated in an incoherent manner, and the atomic spin and probe field occupy the unnormalized quantum states $\rho_B(t)$ which are correlated with the value of the B field. The probability

distribution of the magnetic field is then given by the expectation value of the projection operator $|B\rangle\langle B|$, and has the formal expression $P(B) = \mathrm{tr}[|B\rangle\langle B|\rho(t)] = \mathrm{tr}_r[\rho_B(t)]$, where tr_r denotes the trace over the space of the atomic and field degrees of freedom.

We represent $\rho(t)$ by an effective hybrid classical-quantum Wigner function $W(\mathbf{y})$ with the five arguments $\mathbf{y} = (B, x_{\mathrm{at}}, p_{\mathrm{at}}, x_{\mathrm{ph}}, p_{\mathrm{ph}})^T$, for which the integral over all but one variable yields the marginal distribution for that variable. Due to the linear character of the problem, the Wigner function is Gaussian, and hence it is fully characterized by its mean values $\langle\mathbf{y}\rangle$ and its covariance matrix $\boldsymbol{\gamma}$ with elements $\gamma_{ij} = 2\mathrm{Re}\langle(y_i - \langle y_i\rangle)(y_j - \langle y_j\rangle)\rangle$. We shall now recall the evolution of those quantities under the interactions and the measurement dynamics.

Evolution of mean values and covariance matrix elements

We assume that the time-dependent magnetic field is not known by the observer, who will thus have recourse to a probabilistic description. That is, the Ornstein-Uhlenbeck process is not represented by a stochastic equation, but by its effect on the first and second moments of the Gaussian probability distribution of the field and atomic variables.

Starting from the fully spin-polarized state, the incident linearly polarized field, and prior Gaussian distribution for the magnetic field with zero mean and variance V_b, the joint Gaussian distribution is characterized by the vector of mean values and matrix of covariances

$$\langle\mathbf{y}\rangle = (0, 0, 0, 0, 0), \tag{6}$$

$$\boldsymbol{\gamma} = \mathrm{diag}(2V_b, 1, 1, 1, 1). \tag{7}$$

We partition the 5×5 covariance matrix $\boldsymbol{\gamma}$ and mean value vector $\langle y\rangle$ into blocks,

$$\boldsymbol{\gamma} = \begin{pmatrix} \mathbf{A} & \mathbf{C} \\ \mathbf{C}^T & \mathbf{B} \end{pmatrix}, \tag{8}$$

$$\langle\mathbf{y^T}\rangle = (\mathbf{m^T}, \mathbf{n^T}). \tag{9}$$

Here, $\mathbf{m}$ and $\mathbf{A}$ denote the mean value vector and the 3×3 covariance matrix for the B field and the atomic variables $(B, x_{\mathrm{at}}, p_{\mathrm{at}})^T$, while $\mathbf{n}$ and $\mathbf{B}$ denote the mean value vector and the 2×2 covariance matrix for the field variables $(x_{\mathrm{ph}}, p_{\mathrm{ph}})^T$, and $\mathbf{C}$ denotes the covariances between the optical field observables and the atoms and the B field.

To describe the continuous probing, we note that each light segment approaching the atomic ensemble is not yet correlated with the atoms and the B field, and hence we assume the values

$$\mathbf{B} \to \mathbb{1}_{2\times2}, \tag{10}$$

$$\mathbf{C} \to 0_{3\times2}, \tag{11}$$

$$\mathbf{n} \to 0_{2\times1}, \tag{12}$$

which we insert together with the current covariance matrix $\mathbf{A}$ and mean values $\mathbf{m}$ in (8) and (9), respectively.

The mean value of B is damped by a rate γ_b, which also affects all covariance matrix elements involving B, and the variance of B is furthermore subject to diffusive spreading with rate σ_b. The Hamiltonian (5) similarly causes a linear mixing of the mean values, and a corresponding mixing of the covariance matrix elements.

This leads to the following update rules during a small time interval τ:

$$\langle\mathbf{y}\rangle \to \mathbf{S}\langle\mathbf{y}\rangle, \tag{13}$$

$$\boldsymbol{\gamma} \to \mathbf{S}\boldsymbol{\gamma}\mathbf{S}^T + L, \tag{14}$$

where

$$\mathbf{S} = \begin{pmatrix} 1-\gamma_b\tau & 0 & 0 & 0 & 0 \\ 0 & 1 & 0 & 0 & \kappa\sqrt{\tau} \\ -\mu\tau & 0 & 1 & 0 & 0 \\ 0 & 0 & \kappa\sqrt{\tau} & 1 & 0 \\ 0 & 0 & 0 & 0 & 1 \end{pmatrix}, \tag{15}$$

and $\mathbf{L} = \mathrm{diag}(2\sigma_b\tau, 0, 0, 0, 0)$.

After the interaction, the atoms and the light segment have become correlated, which implies that the covariance matrix has nonvanishing entries between their corresponding components.

The light segment subsequently moves away from the atoms and we may either disregard it, in which case the remaining components are merely described by a Gaussian distribution with mean values $\mathbf{m}$ and covariance matrix $\mathbf{A}$, or we may perform a projective measurement of the photonic quadrature x_{ph} with a random measurement outcome x_{ms} (Gaussian distributed with a mean value n_1 and variance of $1/2$ [26]). Due to the correlations in the Gaussian state, the projective measurement on the optical field updates the mean values and the covariances of the B field and atomic variables according to

$$\mathbf{A} \to \mathbf{A} - \mathbf{C}(\pi\mathbf{B}\pi)^-\mathbf{C}, \tag{16}$$

$$\mathbf{m} \to \mathbf{m} + \mathbf{C}(\pi\mathbf{B}\pi)^-((x_{\mathrm{ms}} - n_1), 0)^T, \tag{17}$$

where $\pi = \mathrm{diag}(1, 0)$ designates that we measure the first of the two light quadratures, and $(\cdot)^-$ denotes the Moore-Penrose pseudoinverse. To lowest order in τ, $(\pi\mathbf{B}\pi)^- = \mathrm{diag}(1, 0)$.

As each segment of the light beam interacts only infinitesimally with the atomic system, the field variables can be eliminated, and to first order in the time increment τ, the dynamics can be expressed in a closed set of equations for the mean values and the covariances of the B field and atomic variables alone. Denoting the matrix elements of $\mathbf{A}$ by a_{ij}, we get the deterministic update rule for $\mathbf{A}$,

$$\mathbf{A} \to \begin{pmatrix} (1-2\gamma_b\tau)a_{11} + 2\sigma_b\tau & (1-\gamma_b\tau)a_{12} & (1-\gamma_b\tau)a_{13} - \mu\tau a_{11} \\ (1-\gamma_b\tau)a_{21} & a_{22} + \kappa^2\tau & a_{23} - \mu\tau a_{21} \\ (1-\gamma_b\tau)a_{31} - \mu\tau a_{11} & a_{32} - \mu\tau a_{12} & a_{33} - \mu\tau(a_{31} + a_{13}) \end{pmatrix} - \kappa^2\tau\begin{pmatrix} a_{13}^2 & a_{13}a_{23} & a_{13}a_{33} \\ a_{13}a_{23} & a_{23}^2 & a_{23}a_{33} \\ a_{13}a_{33} & a_{23}a_{33} & a_{33}^2 \end{pmatrix}. \tag{18}$$
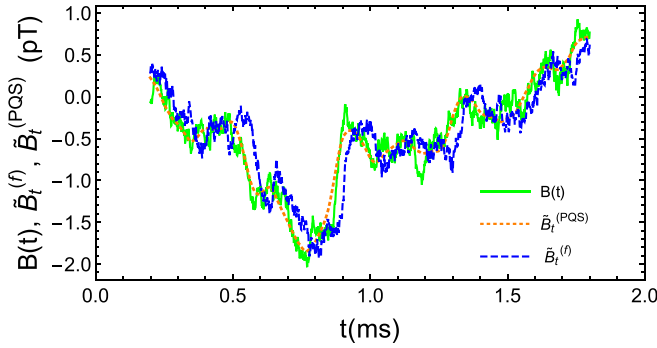
FIG. 2. The solid green curve shows a simulated field $B(t)$, fluctuating according to the Ornstein-Uhlenbeck process (1) with parameters $\gamma_b = 1.0 \times 10^3 \text{ s}^{-1}$, $\sigma_b = 2.0 \times 10^3 \text{ pT}^2/\text{s}$. The magnetic field is coupled with strength $\mu = 2.0 \times 10^5 \text{ s}^{-1}$ to the atomic ensemble, which is coupled with the strength $\kappa^2 = 10^4 \text{ s}^{-1}$ to the optical probe. By conventional forward filtering, the simulated detection record yields the estimate $\tilde{B}_t^{(f)}$ of the magnetic field shown by the dashed blue curve, while the past quantum state (PQS) (smoothing) scheme yields the estimate $\tilde{B}_t^{(\text{PQS})}$ shown by the dotted orange curve.

The expected mean outcome of the field measurement is $\langle x_{\text{ms}} \rangle = n_1 = \kappa \sqrt{\tau} m_3$, and the mean values for the magnetic field and atomic observables, conditioned on a given outcome x_{ms}, are given by

$$\mathbf{m} \rightarrow \begin{pmatrix} (1 - \gamma_b \tau) m_1 \\ m_2 \\ m_3 \end{pmatrix} + \kappa \sqrt{\tau} (x_{ms} - \kappa \sqrt{\tau} m_3) \begin{pmatrix} a_{13} \\ a_{23} \\ a_{33} \end{pmatrix}. \quad (19)$$

Propagating these equations in subsequent steps of duration τ, we acquire or simulate the detection record and determine the conditional dynamics of the atomic quantum state and the estimate $\tilde{B}_t^{(f)}$ of the current value of the magnetic field $B(t)$. This estimate is given by the first component of $\mathbf{m}$, the vector of mean values, which depends on the stochastic detection record. The dynamics of the covariance matrix is deterministic and reaches a steady state irrespective of the measurement outcomes. The collective atomic spin variables and the B field are correlated and the conditional probability distribution for $B(t)$ is a Gaussian with a variance given by half of the first diagonal element of $\mathbf{A}$. This variance is the mean square error, $\langle \Delta^2 \tilde{B}_t^{(f)} \rangle$, of our estimate,

$$\tilde{B}_t^{(f)} = [\mathbf{m}_\rho]_1, \quad (20)$$

$$\langle \Delta^2 \tilde{B}_t^{(f)} \rangle = \tfrac{1}{2} [\mathbf{A}_\rho]_{11}. \quad (21)$$

In Fig. 2, we show a simulated realization of the noisy $B(t)$ (solid green curve). The dashed blue curve shows our estimate $\tilde{B}_t^{(f)}$ by the procedure outlined above. We observe an overall good agreement, but we also note that individual spikes in $B(t)$ are not reproduced, while other spikes appear. This reflects that the data acquisition is not fast enough to resolve rapid changes of $B(t)$, while the measurement shot-noise fluctuations may cause erroneous variations in the magnetic field estimate. Notably, the time dependence of the dashed blue curve lags behind the solid green one. This is because changes in $B(t)$ are accumulated over time in the value of the

spin precession angle and are only reliably discerned after a suitable optical signal has been obtained.

IV. RETRODICTION OF THE MAGNETIC FIELD AND ATOMIC STATE

In the previous section, we determined the joint Gaussian probability distribution of the magnetic field and the atomic collective spin at time t, conditioned on the probing data obtained until time t. In the quantum theory of measurements, each interaction and probing event with outcome m_i is formally described by a positive operator-valued measure (POVM) element, and the full optical detection process of our scheme is described by applying a sequence of operators M_{m_i}, including both the deterministic time evolution of the state and the evolution conditioned on the measurement outcomes m_i. The joint probability for the occurrence of the full sequence of measurement outcomes is the trace of the corresponding operator product, $P(m_1, m_2, \ldots, m_N) = \text{tr}[M_{m_N} \ldots M_{m_1} \rho(0) M_{m_1}^\dagger \ldots M_{m_N}^\dagger]$, while the joint probability of all measurement outcomes *and* a projective measurement of the magnetic field yielding the value B at an intermediate time t reads $P(m_1, m_2, \ldots, B_t, \ldots, m_N) = \text{tr}[M_{m_N} \ldots |B\rangle\langle B| \ldots M_{m_1} \rho(0) M_{m_1}^\dagger \ldots |B\rangle\langle B| \ldots M_{m_N}^\dagger]$.

Note that if the optical probing stops just before time t, the conditional quantum state at this time reads $\rho(t) \propto M_{m_N} \ldots M_{m_1} \rho(0) M_{m_1}^\dagger \ldots M_{m_N}^\dagger$ and the inferred conditional probability agrees with the conventional Born rule, $P(B) = \text{tr}[|B\rangle\langle B| \rho(t)]$. In the case of continued probing *after* t, we can use the cyclic property of the trace and reorganize terms to write the joint probability distributions as $P(m_1, m_2, \ldots B_t, \ldots, m_N) = \text{tr}[|B\rangle\langle B|(\ldots M_{m_1} \rho(0) M_{m_1}^\dagger \ldots)|B\rangle\langle B|(\ldots M_{m_N}^\dagger M_{m_N} \ldots)]$.

Since the outcomes m_i are the ones actually measured, we infer the probability that the magnetic field would have been projectively measured to have the value B, conditioned on all prior and posterior detection events to be proportional to $\text{tr}[|B\rangle\langle B| \rho(t)|B\rangle\langle B| E(t)]$ [21], with $\rho(t) = [\ldots M_{m_1} \rho(0) M_{m_1}^\dagger \ldots]$ and $E(t) = (\ldots M_{m_N}^\dagger M_{m_N} \ldots)$, where the $\ldots$ in the expressions for $\rho(t)$ and $E(t)$ represent the sequences of POVM elements, until and after the time t, respectively.

A. Backward evolution of the effect operator

The POVM operators for optical probing can be determined as integrals with Gaussian kernels (see, e.g., [27]), but we shall have recourse to a simplified argument that utilizes the more convenient representation of the operators $\rho(t)$ and $E(t)$ in terms of Gaussian mean values and covariance matrices. This representation applies because both operators are evolved by Gaussian preserving elements and hence both have Gaussian Wigner functions [any operator on an effective position and momentum operator phase space has a Wigner function representation, and being a Hermitian and positive operator, $E(t)$ has a Wigner function with similar properties as the one of a conventional quantum state $\rho(t)$]. Indeed, the time evolution of the ρ and the E operators are equivalent, except that $E(t)$ evolves from the later towards the earlier times. As a consequence, $E(t)$ is described by a Gaussian

Wigner function, and its first and second moments evolve with similar factors as the moments for $\rho(t)$.

We describe $E(t)$ by a covariance matrix $\boldsymbol{\gamma}_E(t)$ and a vector of mean values, $\langle \mathbf{y}_E \rangle = (\mathbf{m}_E, \mathbf{n}_E)$, for which the evolution from $t + \tau$ to t yields

$$\langle \mathbf{y}_E \rangle \rightarrow \mathbf{S}_E \langle \mathbf{y}_E \rangle, \tag{22}$$

$$\boldsymbol{\gamma}_E \rightarrow \mathbf{S}_E \boldsymbol{\gamma}_E \mathbf{S}_E^T + L, \tag{23}$$

where

$$\mathbf{S}_E = \begin{pmatrix} 1 + \gamma_b \tau & 0 & 0 & 0 & 0 \\ 0 & 1 & 0 & 0 & -\kappa\sqrt{\tau} \\ \mu\tau & 0 & 1 & 0 & 0 \\ 0 & 0 & -\kappa\sqrt{\tau} & 1 & 0 \\ 0 & 0 & 0 & 0 & 1 \end{pmatrix}, \tag{24}$$

and $\mathbf{L} = \mathrm{diag}(2\sigma_b\tau, 0, 0, 0, 0)$.

Going through the matrix multiplications and eliminating the optical field components, we obtain the deterministic evolution of the magnetic field and atomic components covariance matrix, backward in time from $t + \tau$ to t for the operator $E(t)$.

Denoting the matrix elements of $\mathbf{A}_E$ by a_{ij}, we get the deterministic update rule for $\mathbf{A}_E$,

$$\mathbf{A}_E \rightarrow \begin{pmatrix} (1 + 2\gamma_b\tau)a_{11} + 2\sigma_b\tau & (1 + \gamma_b\tau)a_{12} & (1 + \gamma_b\tau)a_{13} + \mu\tau a_{11} \\ (1 + \gamma_b\tau)a_{21} & a_{22} + \kappa^2\tau & a_{23} + \mu\tau a_{21} \\ (1 + \gamma_b\tau)a_{31} + \mu\tau a_{11} & a_{32} + \mu\tau a_{22} & a_{33} + \mu\tau(a_{31} + a_{13}) \end{pmatrix} - \kappa^2\tau \begin{pmatrix} a_{13}^2 & a_{13}a_{23} & a_{13}a_{33} \\ a_{13}a_{23} & a_{23}^2 & a_{23}a_{33} \\ a_{13}a_{33} & a_{23}a_{33} & a_{33}^2 \end{pmatrix}. \tag{25}$$

The centroid of the Gaussian Wigner function for $E(t)$ depends on the measurement outcome x_{ms} and is given by

$$\mathbf{m}_E \rightarrow \begin{pmatrix} (1 + \gamma_b\tau)m_1 \\ m_2 \\ m_3 \end{pmatrix} + \kappa\sqrt{\tau}(x_{\mathrm{ms}} + \kappa\sqrt{\tau}m_3) \begin{pmatrix} a_{13} \\ a_{23} \\ a_{33} \end{pmatrix}, \tag{26}$$

where we emphasize that in these equations, the matrix and vector elements a_{ij}, m_i are the ones pertaining to $\mathbf{A}_E$ and $\mathbf{m}_E$, and not to $\mathbf{A}_\rho \equiv \mathbf{A}$ and $\mathbf{m}_\rho \equiv \mathbf{m}$ in (18) and (19).

B. Past quantum state estimate of the time-dependent magnetic field

Given the first and second moments of Gaussian states, we have the information needed to construct the $\rho(t)$ and $E(t)$ matrices, and may thus, in principle, determine the probability distribution for the outcomes of any measurement process at time t conditioned on all previous and later measurements. The evaluation of arbitrary operator expressions from Wigner functions is, however, not a trivial one, and to avoid a cumbersome translation between operator expressions and their Wigner function phase-space equivalents, we shall employ arguments to arrive at the desired result directly in terms of the conditional mean values and covariance matrices.

First, we note that $\mathrm{tr}_B(|B\rangle\langle B|\rho) = \langle B|\rho|B\rangle$ and $\mathrm{tr}_B(|B\rangle\langle B|E) = \langle B|E|B\rangle$, where tr_B denotes the partial trace over the B degree of freedom, are operators on the atomic spin Hilbert space. This leads to the observation that

$$P_{\mathrm{PQS}}(B) \propto \mathrm{tr}(|B\rangle\langle B|\rho|B\rangle\langle B|E)$$
$$\mathrm{tr}_r \langle B|\rho|B\rangle \langle B|E|B\rangle, \tag{27}$$

where tr_r denotes the reduced trace over the atomic collective spin (oscillator) variables. The trace of a product of operators (a scalar product on the space of operators) equals 2π times the phase-space integral of the product of the corresponding Wigner functions. Hence, we obtain

$$P_{\mathrm{PQS}}(B) \propto \int dx_{\mathrm{at}} dp_{\mathrm{at}} W_\rho(B, x_{\mathrm{at}}, p_{\mathrm{at}}) W_E(B, x_{\mathrm{at}}, p_{\mathrm{at}}). \tag{28}$$

We now use the fact that the Wigner functions are Gaussian distributions and write their product explicitly as

$$\Pi_{\rho,E}(B, x_{\mathrm{at}}, p_{\mathrm{at}}) = W_\rho(B, x_{\mathrm{at}}, p_{\mathrm{at}}) W_E(B, x_{\mathrm{at}}, p_{\mathrm{at}})$$
$$\propto e^{-(\mathbf{y}-\mathbf{m}_\rho)^T \mathbf{A}_\rho^{-1}(\mathbf{y}-\mathbf{m}_\rho)} e^{-(\mathbf{y}-\mathbf{m}_E)^T \mathbf{A}_E^{-1}(\mathbf{y}-\mathbf{m}_E)}, \tag{29}$$

where $\mathbf{y} = (B, x_{\mathrm{at}}, p_{\mathrm{at}})^T$, $\mathbf{m}_{\rho(E)}$ denote the displaced mean values, and $\mathbf{A}_{\rho(E)}$ are the 3×3 covariance matrices of the magnetic field and atomic spin components of $\mathbf{y}$, in the Gaussian distributions $W_{\rho(E)}$. After elementary algebra, we can rewrite the product $\Pi_{\rho,E}$ in a single Gaussian form,

$$\Pi_{\rho,E} \propto e^{-(\mathbf{y}-\mathbf{m}_{\rho,E})^T \mathbf{A}_{\rho,E}^{-1}(\mathbf{y}-\mathbf{m}_{\rho,E})}, \tag{30}$$

with the new covariance matrix $\mathbf{A}_{\rho,E}$ and mean value $\mathbf{m}_{\rho,E}$ given by

$$\mathbf{A}_{\rho,E}^{-1} = \mathbf{A}_\rho^{-1} + \mathbf{A}_E^{-1}, \tag{31}$$

$$\mathbf{m}_{\rho,E} = \mathbf{A}_{\rho,E}(\mathbf{A}_\rho^{-1}\mathbf{m}_\rho + \mathbf{A}_E^{-1}\mathbf{m}_E). \tag{32}$$

Therefore, in the PQS framework, the estimated magnetic field and variance of its conditional distribution are given by the first vector component and matrix element,

$$\tilde{B}_{\mathrm{t}}^{(\mathrm{PQS})} = [(\mathbf{A}_\rho^{-1} + \mathbf{A}_E^{-1})^{-1}(\mathbf{A}_\rho^{-1}\mathbf{m}_\rho + \mathbf{A}_E^{-1}\mathbf{m}_E)]_1, \tag{33}$$

$$\langle \Delta^2 \tilde{B}_{\mathrm{t}}^{(\mathrm{PQS})} \rangle = \tfrac{1}{2}[(\mathbf{A}_\rho^{-1} + \mathbf{A}_E^{-1})^{-1}]_{11}. \tag{34}$$

Equations (33) and (34), together with the equations to determine their constituents, are the main results of this article. Given the probing record, they yield a Bayesian estimate of the time-dependent magnetic field strength in the form of a Gaussian distribution, where $\tilde{B}_{\mathrm{t}}^{(\mathrm{PQS})}$ is the estimate that has the smallest mean-squared error $\langle \Delta^2 \tilde{B}_{\mathrm{t}}^{(\mathrm{PQS})} \rangle$ with respect to the actual value $B(t)$. In Fig. 2, the dotted orange curve shows the value of the PQS estimator given by Eq. (33) for the given detection record. $\tilde{B}_{\mathrm{t}}^{(\mathrm{PQS})}$, indeed, follows the true value (the solid green curve) of the simulated magnetic field $B(t)$ generated by the OU process (1) fairly well. Due to the use of the entire detection record in the estimate of the field at any time t, the estimate follows monotonic increases and decreases better
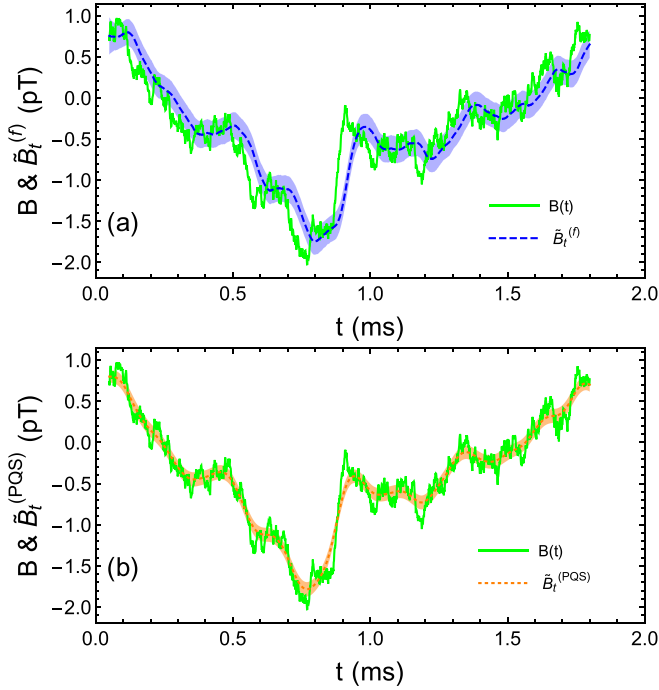
FIG. 3. The two panels show how well a given time-dependent B field (solid green curves) is estimated in 2000 independent simulations of the optical detection. (a) The blue band represents the mean value and standard deviation of the quantum filter estimates. (b) The orange band shows the mean value and standard deviation of the time-dependent PQS estimator.

than the filter theory, while upward and downward spikes in $B(t)$ that are not well resolved by the optical probing cannot be inferred from previous and later data. In the next section we shall more quantitatively address the performance of the forward filter and the past quantum state estimation.

V. PERFORMANCE OF FILTER AND PQS ESTIMATES

We have applied the quantum filtering and the PQS formalism to estimate a time-dependent stochastic magnetic field from the optical probe signal. The example in Fig. 2 clearly shows that the estimates $\tilde{B}_t^{(f)}$ and $\tilde{B}_t^{(PQS)}$ approximately follow the true value of the field $B(t)$. We also observe that $\tilde{B}_t^{(PQS)}$ is smoother than $\tilde{B}_t^{(f)}$. While causing backaction on the mean value vectors $\mathbf{m}_\rho$ ($\mathbf{m}_E$) as the time argument passes from t to $t + \tau$ (from $t + \tau$ to t), the stochastic contribution of the photon shot noise to the measurement outcome in the intervening interval merely changes from having an influence on $E(t + \tau)$ to $\rho(t + \tau)$. This partly suppresses its effect on the estimate (33) based on both ρ and E. While $\tilde{B}_t^{(f)}$ (the dashed blue curve in Fig. 2) visibly lags behind decreases and increases in the true field $B(t)$ (the solid green curve), $\tilde{B}_t^{(PQS)}$ (the dotted orange curve) performs well under such variations, but it fails to resolve spikes in the true magnetic field $B(t)$.

To characterize the quantitative performance of our estimators, we have simulated $M = 2000$ independent realizations of the optical measurements on an atomic sample subject to the same realization of the magnetic field $B(t)$. Figure 3(a) shows the time-dependent average of the quantum filter es-

timator, where the half width of the blue band indicates the standard deviation of the estimates (around their mean value) due to photon shot noise. Figure 3(b) shows the corresponding average time dependence and standard deviation for the PQS estimator. These calculations clearly confirm the quantitative superiority of the PQS estimator, but they also display the systematic, average bias of the two methods.

The standard deviations shown by the blue and orange bands in the figure do not represent the fluctuations of the estimated field around the true $B(t)$, but our numerical simulations allow us to quantitatively address the quality of the filter and PQS estimates. We can thus use our simulations to evaluate the mean-squared error (MSE),

$$\text{MSE}(t) = \frac{1}{M} \sum_{k=1}^{M} [\tilde{B}_{t,k}^{(X)} - B(t)]^2, \qquad (35)$$

where $\tilde{B}_{t,k}^{(X)}$ represents the filter estimate (20) for $X = f$ and the PQS estimate (33) for $X = \text{PQS}$.

In Fig. 4, the noisy thin blue (upper) and orange (lower) curves show the MSE of the quantum filter and the PQS estimator, respectively. The lower envelope of these noisy curves shows the variances of the estimators (around the estimator mean values) represented by the width of the blue and orange curves in Figs. 3(a) and 3(b), respectively. They have almost constant values and suggest that the MSE has an almost time-independent contribution from the fluctuations due to the photon shot noise, while the time-dependent bias of the mean estimators, $\overline{B}(t) = \frac{1}{M} \sum_{k=1}^{M} \tilde{B}_{t,k}^{(X)}$, is correlated with the increases and decreases or the spikes of the true field $B(t)$ and yields a main contribution to the estimation error, $\text{MSE}(t) = \frac{1}{M} \sum_{k=1}^{M} [\tilde{B}_{t,k}^{(X)} - \overline{B}(t)]^2 + [\overline{B}(t) - B(t)]^2$. Indeed, the broad maxima in the thin blue curve in Fig. 4(a) occur when the true field is increasing or decreasing in Fig. 3, while the maxima of the thin orange curve in Fig. 4(b) coincide with the spikes of the true field.

The thin dotted lines show the average MSE for the quantum filter and the PQS estimator over 2000 independent realizations of $B(t)$. As the fluctuations in $B(t)$ occur at random times, the average MSE is constant in time up to fluctuations due to the finite sample. For comparison, the dashed line segments in the right-hand side of the figure show the variances of the Gaussian distributions, identified by our deterministic theory for the covariance matrix for ρ and for both ρ and E. These are identical with the results of the forward Kalman-Bucy filter and the forward and backward filters combined in the Mayne-Fraser-Potter two-filter smoother [12,13]. Our numerical calculations confirm that the average MSE of the quantum filter and the PQS estimates are both correctly determined by the covariance matrix. The reduction in the mean-squared error by the PQS analysis is substantial and, in Fig. 5, we compare the filter and PQS methods as function of the timescale of the Ornstein-Uhlenbeck process γ_b and the probing strength κ^2. With a given, finite probing strength κ^2, the time evolution of the magnetic field is tracked progressively better by both methods when $\gamma_b < \kappa^2$. It is in the same regime that the PQS advantage over forward filtering is maximal.
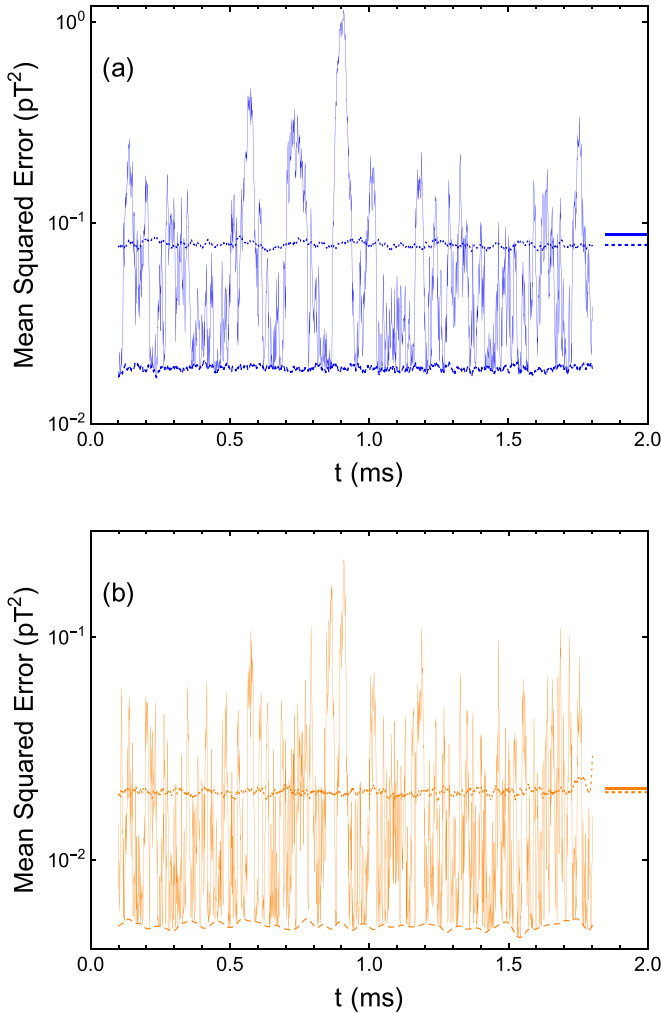
FIG. 4. The (a) thin blue and (b) orange curves show the mean-squared error (MSE) of 2000 simulations of the quantum filter and PQS estimates for the true time-dependent magnetic field shown in Fig. 3. The dashed lower envelopes of the mean-squared error show the almost constant variance of the estimators (over the 2000 simulated experiments). The dotted lines indicate the ensemble-averaged mean-squared error over 2000 different realizations of $B(t)$. The values depicted by the dashed line segments in the right-hand side of the figure show the variances given by Eqs. (21) and (34), following from our Gaussian-state formalism in the previous sections. These agree perfectly with the ensemble-averaged mean-squared error, and, to within the expected variation, they also agree with the time average of the thin blue and orange curves, i.e., the MSE for a single realization of $B(t)$, shown as the solid line segments.

VI. DISCUSSION

In this paper, we have developed a theory based on the quantum filtering and PQS schemes for the estimation of a time-dependent magnetic field generated by an Ornstein-Uhlenbeck process. Our numerical simulation results confirm and explain an enhanced precision of the estimate of the time-dependent magnetic field by full measurement records over the conventional quantum filtering approach. While we studied a very specific and idealized model, it is readily possible within the Gaussian formalism to incorporate extra
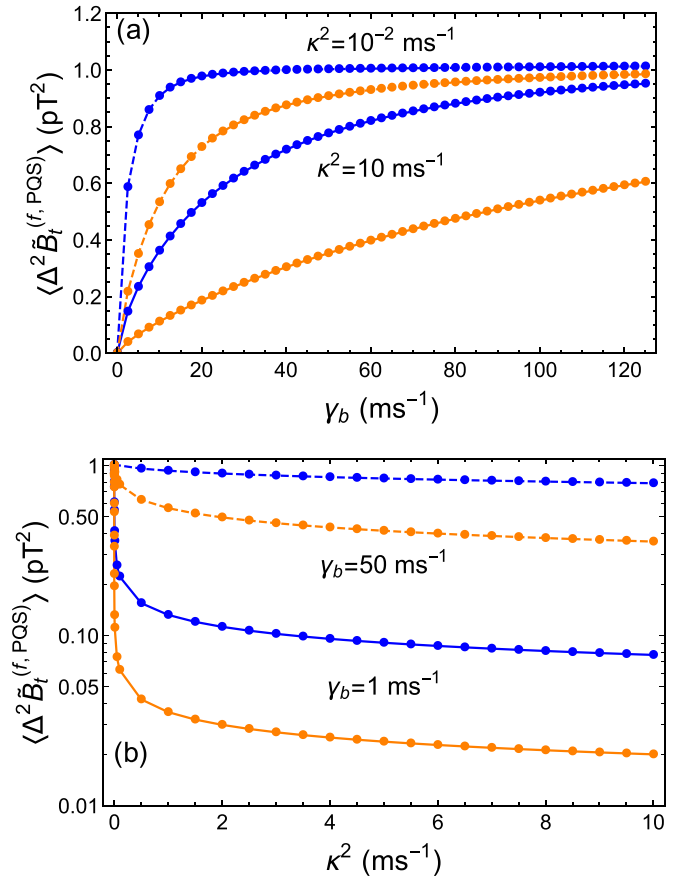

FIG. 5. The theoretically determined variances of the conditional Gaussian distribution for B are shown as a function of (a) γ_b and (b) κ^2. The blue curves (numbers 1 and 3 from the top of the panel) represent the filtering process, while the orange curves (numbers 2 and 4) describe the PQS scheme. Dots indicate numerical data and lines are guides to the eye. In (a), we assume fixed values of $\kappa^2 = 10^{-2}$ ms^{-1} (upper dashed blue and orange lines) and $\kappa^2 = 10$ ms^{-1} (lower solid blue and orange lines). In (b), we assume fixed value of $\gamma_b = 1.0$ ms^{-1} (upper dashed blue and orange lines) and $\gamma_b = 50.0$ ms^{-1} (lower solid blue and orange lines). In both panels, $\sigma_b/\gamma_b = 1$ pT^2 and $\mu = 200$ ms^{-1}.

dissipative terms and treat inhomogeneities in the system by more degrees of freedom [9], to study other linear couplings such as exchange of oscillator quanta between the system and the probe, and to employ squeezing and phase-sensitive amplification to the probe field [28].

Our hybrid quantum-classical theory is equivalent to the classical theory of Kalman filtering and smoothing on the one hand, and with the theory of quantum trajectories and past quantum states on the other hand. We believe that the combined insight from these two domains of precision metrology may play a crucial role and may point to the use of further theoretical methods in the very active field of high-precision measurements and hypothesis testing with quantum systems.

[1] V. Giovannetti, S. Lloyd, and L. Maccone, Science **306**, 1330 (2004).

[2] I. K. Kominis, T. W. Kornack, J. C. Allred, and M. V. Romalis, Nature (London) **422**, 596 (2003).

[3] L. K. Thomsen, S. Mancini, and H. M. Wiseman, Phys. Rev. A **65**, 061801(R) (2002).

[4] P. S. Maybeck, *Stochastic Models, Estimation, and Control, Volume 1* (Academic Press, New York, 1979).

[5] J. M. Geremia, J. K. Stockton, A. C. Doherty, and H. Mabuchi, Phys. Rev. Lett. **91**, 250801 (2003).

[6] R. Jimenez-Martinez, J. Kolodynski, C. Troullinou, V. G. Lucivero, J. Kong, and M. W. Mitchell, Phys. Rev. Lett. **120**, 040503 (2018).

[7] J. K. Stockton, J. M. Geremia, A. C. Doherty, and H. Mabuchi, Phys. Rev. A **69**, 032109 (2004).

[8] K. Mølmer, and L. B. Madsen, Phys. Rev. A **70**, 052102 (2004).

[9] L. B. Madsen and K. Mølmer, Phys. Rev. A **70**, 052324 (2004).

[10] V. Petersen and K. Mølmer, Phys. Rev. A **74**, 043802 (2006).

[11] A. Aravkin, J. V. Burke, L. Ljung, A. Lozano, and G. Pillonetto, arXiv:1609.06369.

[12] M. Tsang, Phys. Rev. Lett. **102**, 250403 (2009).

[13] M. Tsang, Phys. Rev. A **80**, 033840 (2009).

[14] M. Tsang, Phys. Rev. A **81**, 013824 (2010).

[15] M. Tsang, J. H. Shapiro, and S. Lloyd, Phys. Rev. A **78**, 053820 (2008).

[16] M. Tsang, J. H. Shapiro, and S. Lloyd, Phys. Rev. A **79**, 053843 (2009).

[17] V. P. Belavkin, J. Phys. A: Math. Gen. **22**, L1109 (1989); Phys. Lett. A **140**, 355 (1989).

[18] H. Carmichael, *An Open Systems Approach to Quantum Optics*, Lecture Notes in Physics Series (Springer-Verlag, Berlin, 1993).

[19] J. Dalibard, Y. Castin, and K. Mølmer, Phys. Rev. Lett. **68**, 580 (1992).

[20] S. Gammelmark and K. Mølmer, Phys. Rev. Lett. **112**, 170401 (2014).

[21] S. Gammelmark, B. Julsgaard, and K. Mølmer, Phys. Rev. Lett. **111**, 160401 (2013).

[22] W. H. Press, S. A. Teukolsky, W. T. Vetterling, and B. P. Flannery, Numerical recipes, *The Art of Scientific Computing*, 3rd ed. (Cambridge University Press, New York, 2007).

[23] M. Greenfeld, D. S. Pavlichin, H. Mabuchi, and D. Herschlag, PLoS ONE **7**, e30024 (2012).

[24] S. Gammelmark, K. Mølmer, W. Alt, T. Kampschulte, and D. Meschede, Phys. Rev. A **89**, 043839 (2014).

[25] J. Sherson, B. Julsgaard, and E. S. Polzik, Adv. At. Mol. Opt. Phys. **54**, 81 (2007).

[26] In the analysis of a real experimental record, x_{ms} is the actual measurement outcome, while to simulate an experiment, we evolve only the atomic and photonic components of Eqs. (6)–(17) subject to a given stochastic realization of $B(t)$ according to the OU process. We then choose x_{ms} at random at each time step, according to a Gaussian distribution with mean value n_1 and variance $1/2$.

[27] H. Bao, J. L. Duan, X. D. Lu, P. X. Li, W. Z. Qu, S. C. Jin, M. F. Wang, I. Novikova, E. Mikhailov, K. F. Zhao, K. Mølmer, H. Shen, and Y. H. Xiao, Nature (London) **581**, 159 (2020).

[28] V. Petersen, L. B. Madsen, and K. Mølmer, Phys. Rev. A **72**, 053812 (2005).